

# Finite size of hadrons and HBT interferometry for hydrodynamic sources

Yong Zhang<sup>1,2\*</sup>, Hong-Jie Yin<sup>3</sup>, and Weihua Wu<sup>1</sup>

<sup>1</sup>*School of Mathematics and Physics,  
Jiangsu University of Technology,  
Changzhou, Jiangsu 213001, China*

<sup>2</sup>*School of Science,  
Inner Mongolia University of Science & Technology, Baotou,  
Inner Mongolia Autonomous Region 014010, China*

<sup>3</sup>*College of Mathematics and Physics,  
Bohai University, Jinzhou, Liaoning 121013, China*

(Dated: June 25, 2019)

Hadrons formed in heavy-ion collisions are not point-like objects, they cannot occupy too close space-time points. When the two bosons are too close to each other, their constituents start to mix and they cannot be considered as bosons subjected to Bose-Einstein statistics, this effect is called excluded volume effect. We study the volume effect on HBT for the sources with various sizes. The effect on HBT was shown in out, side and long directions, and it is more obvious for the source with a narrow space-time distribution. The correlation functions for high transverse momenta are more suppressed by the volume effect. Hence the incoherence parameter may be more suppressed by the volume effect for high transverse momenta in small collision systems.

Keywords: heavy-ion collisions, HBT interferometry, excluded volume effect.

PACS numbers: 25.75.Dw, 25.75.Gz

## I. INTRODUCTION

Hanbury-Brown-Twiss (HBT) interferometry has become an important tool for detecting the space-time structure of the particle emitting sources formed in heavy-ion collisions [1–4]. The correlation functions of two identical bosons were defined as the ratio of the two-particle momentum spectrum  $N(\mathbf{k}_1, \mathbf{k}_2)$  of identical bosons to the product of the two single boson momentum spectra  $N(\mathbf{k}_1)N(\mathbf{k}_2)$ , and the theoretical results of HBT are always above 1. However, the observed data show that the two-pion Bose-Einstein correlations function takes values below unity [5–8].

Hadrons formed in heavy-ion collisions are not point-like objects, they cannot get too close to each other, this effect is called excluded volume effect [9–11]. When the two bosons are too close to each other, their constituents start to mix and they cannot be considered as bosons subjected to Bose-Einstein statistics, so the HBT experiment cannot see two bosons which are too close in space-time [12–14]. In Ref. [12], A. Bialas *et al.* first study the excluded volume effect on HBT. Then the full Bose-Einstein correlation functions was shown in three directions (out,side,long) for pp collisions at 7 TeV [13], using the blast-wave model [15–17]. The excluded volume effect on HBT relates to the size of hadrons and the scale of sources.

In this paper, we study the excluded volume effect on HBT for the sources with various sizes, using the ideal relativistic hydrodynamics in 2+1 dimensions to describe

the transverse expansion of sources with zero net baryon density and combine the Bjorken boost-invariant hypothesis [18] for the source longitudinal evolution. In the calculations, we use the equation of state of s95p-PCE, which combines the hadron resonance gas at low temperatures and the lattice QCD results at high temperatures [19]. We assume that the system reaches the static local equilibrium at  $\tau_0 = 0.6$  fm/c after the collision and take the initial energy density distribution in the transverse plane as the Gaussian distribution,

$$\epsilon = \frac{\epsilon_0}{2\pi R_x R_y} \exp[-x^2/(2R_x^2) - y^2/(2R_y^2)], \quad (1)$$

where  $\epsilon_0$  and  $R_i$  ( $i = x, y$ ) are the parameters of the initial source energy density and radii.

The rest of this paper is organized as follows. In Sec. II, we present the calculating formula of two-pion correlation function for hydrodynamic sources. In Sec. III, we show the excluded volume effect on pion HBT. Finally, a summary and conclusion of this paper are given in Sec. IV.

## II. CALCULATIONS OF HBT FOR HYDRODYNAMIC SOURCES

The Bose-Einstein correlation function was usually defined as [2–4]

$$\begin{aligned} C(\mathbf{k}_1, \mathbf{k}_2) &= \frac{N(\mathbf{k}_1, \mathbf{k}_2)}{N(\mathbf{k}_1)N(\mathbf{k}_2)} \\ &= 1 + \frac{|\int d^4r S(r, K) e^{iq \cdot r}|^2}{\int d^4r_1 S(r_1, k_1) \int d^4r_2 S(r_2, k_2)}, \end{aligned} \quad (2)$$

\*zhy913@jsut.edu.cn

where  $S(r, k)$  is the emission function.  $k_1, r_1$  and  $k_2, r_2$  are momenta and positions of the particles.  $q = k_1 - k_2$ ,  $K = (k_1 + k_2)/2$  are the relative momentum and pair momentum of two identical particles, respectively. With the “smooth assumption”  $S(r, (k_1 + k_2)/2) \approx S(r, k_1) \approx S(r, k_2)$ , the Bose-Einstein correlation function can be rewritten as [4, 20–22]

$$C_0(\mathbf{k}_1, \mathbf{k}_2) = 1 + \frac{\int d^4r_1 d^4r_2 S(r_1, k_1) S(r_2, k_2) \cos(q \cdot (r_1 - r_2))}{\int d^4r_1 S(r_1, k_1) d^4r_2 S(r_2, k_2)}. \quad (3)$$

Considering the excluded volume effect, the HBT correlation function becomes [12–14]

$$C_v(\mathbf{k}_1, \mathbf{k}_2) = C_0(\mathbf{k}_1, \mathbf{k}_2) - C_c(\mathbf{k}_1, \mathbf{k}_2), \quad (4)$$

the corrected part of the correlation function  $C_c(\mathbf{k}_1, \mathbf{k}_2)$  was defined as [13]

$$C_c(\mathbf{k}_1, \mathbf{k}_2) = C_c^{(0)}(\mathbf{k}_1, \mathbf{k}_2) + C_c^{(q)}(\mathbf{k}_1, \mathbf{k}_2), \quad (5)$$

$$C_c^{(0)}(\mathbf{k}_1, \mathbf{k}_2) = \frac{\int d^4r_1 d^4r_2 S(r_1, k_1) S(r_2, k_2) D_{12}}{\int d^4r_1 S(r_1, k_1) d^4r_2 S(r_2, k_2)}, \quad (6)$$

$$C_c^{(q)}(\mathbf{k}_1, \mathbf{k}_2) = \frac{\int d^4r_1 d^4r_2 S(r_1, k_1) S(r_2, k_2) \cos(q \cdot (r_1 - r_2)) D_{12}}{\int d^4r_1 S(r_1, k_1) d^4r_2 S(r_2, k_2)}, \quad (7)$$

where  $D_{12}$  is the cut-off function. For hydrodynamic sources, we treat the cut-off function as

$$D_{12} = e^{-d^2(r_1, r_2)/\Delta r^2 - d^2(t_1, t_2)/\Delta t^2}, \quad (8)$$

where  $d^2(r_1, r_2) = (x_1 - x_2)^2 + (y_1 - y_2)^2 + (z_1 - z_2)^2$  and  $d^2(t_1, t_2) = (t_1 - t_2)^2$  are the total distance and time difference between two particles, respectively. The cut-off distance  $\Delta r \approx 2r_V$  (where  $r_V$  is the radius of the “excluded volume” [9–11, 23] occupied by one pion) was taken to be 1 fm [13]. The cut-off time difference  $\Delta t$  is newly introduced in this study, and it represents the time required for two particles to leave the overlap region. The cut-off time difference  $\Delta t$  is treated as a constant parameter, and it is taken to be 0.2 fm/c in this paper. It can be seen from the Eq. (4)–(7), the volume effect on the correlation function is sensitive to the space-time distribution of the pion source, which will be larger for a narrow space-time distribution of the pion source.

On the freeze-out surface of hydrodynamic sources, the pion emission function is defined by the Cooper-Frye integral [24–27]

$$S(r, p) = \frac{1}{(2\pi)^3} \int_{\Sigma} \frac{p^\mu d^3\sigma_\mu(r') \delta^4(r - r')}{\exp[p^\mu u_\mu(r')/T] - 1}. \quad (9)$$

Where  $u_\mu(r)$  is the flow velocity profiles along the freeze-out surface  $\Sigma$ , and  $d^3\sigma_\mu(r)$  is the outward pointing normal vector on  $\Sigma$  at point  $r$ . The pion freeze-out temperature  $T$  is taken to be 130 MeV [28] in this paper.

### III. RESULTS

#### A. Pion emission source

In Fig. 1, we show the space-time distributions of the freeze-out points of pion in the  $z = 0$  plane for various initial conditions. Where the  $\tau$  and the  $r_\perp$  are the time and the transverse coordinate, respectively, in the  $z = 0$  plane. For a fixed  $\epsilon_0$ , the spatial distribution of the pion source for  $R_x = R_y = 2$  fm is wider than for  $R_x = R_y = 1$  fm, and the emission time of pion for  $R_x = R_y = 2$  fm is earlier than  $R_x = R_y = 1$  fm.

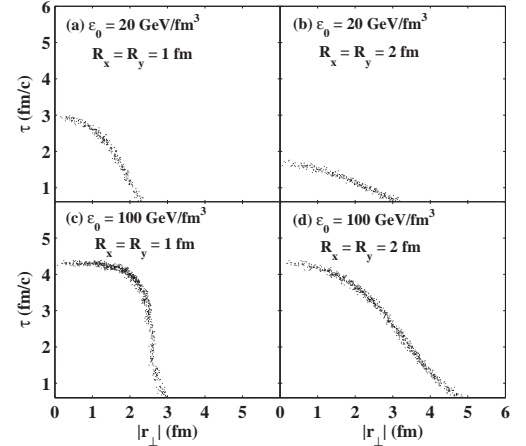


FIG. 1: Distributions of the freeze-out points of pion in the  $z = 0$  plane for various initial conditions.

TABLE I: Spatio-temporal properties of pion emission source. Where the initial conditions (a)–(d) are the same as in Fig. 1.

Initial condition	$\bar{\tau}$ (fm/c)	$\overline{ r_\perp }$ (fm)	$\sigma_\tau$ (fm/c)	$\sigma_r$ (fm)
(a)	2.07	1.37	0.67	0.53
(b)	1.14	1.94	0.30	0.76
(c)	3.60	1.85	0.94	0.65
(d)	2.82	2.66	1.09	1.10

In table I, we show some spatio-temporal properties of pion emission source. Where the initial conditions (a)–(d) are the same as in Fig. 1.  $\bar{\tau}$  and  $\overline{|r_\perp|}$  are the average time and the average transverse radius, respectively, of pion freeze-out points in the  $z = 0$  plane.  $\sigma_\tau$  and  $\sigma_r$  are the standard deviation of the freeze-out time and transverse radius:

$$\sigma_\tau = \sqrt{\frac{1}{N} \sum_{i=1}^N (\tau_i - \bar{\tau})^2}, \quad (10)$$

$$\sigma_r = \sqrt{\frac{1}{N} \sum_{i=1}^N (|r_\perp|_i - \overline{|r_\perp|})^2}. \quad (11)$$

Where  $N$  is the total number of the freeze-out points.  $\tau_i$  and  $|r_\perp|_i$  are the space-time coordinate of the freeze-out point denoted by  $i$ . The  $\sigma_\tau$  and  $\sigma_r$  can represent the width of the space-time distributions of the pion freeze-out points in the  $z = 0$  plane. For fixed initial radius, the width increase with the increasing initial energy density  $\epsilon_0$ .

### B. HBT results

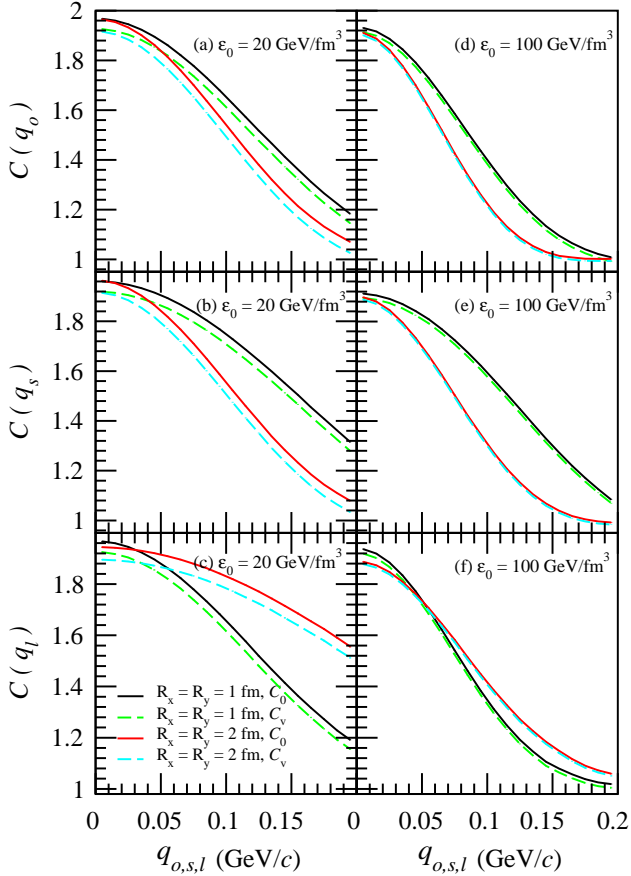


FIG. 2: Correlation function for out (top panel), side (middle panel) and long direction (bottom panel) in the interval  $0.2 \text{ GeV}/c \leq K_T \leq 0.4 \text{ GeV}/c$ . For a fixed direction, the relative momentum  $q$  for other two directions are less than  $40 \text{ MeV}/c$ . Where  $C_0$  is the correlation function without the volume effect, and the  $C_v$  is the correlation function with the volume effect.

In Fig. 2, we show the correlation function for out (top panel), side (middle panel) and long direction (bottom panel) in the interval  $0.2 \text{ GeV}/c \leq K_T \leq 0.4 \text{ GeV}/c$ . For a fixed direction, the relative momentum  $q$  for other two directions are less than  $40 \text{ MeV}/c$ . In the calculations, we take the spatial rapidity  $\eta_s$  in the region  $(-1, 1)$ . Here,  $C_0$  is the correlation function without the volume effect, and the  $C_v$  is the correlation function with the volume

effect.

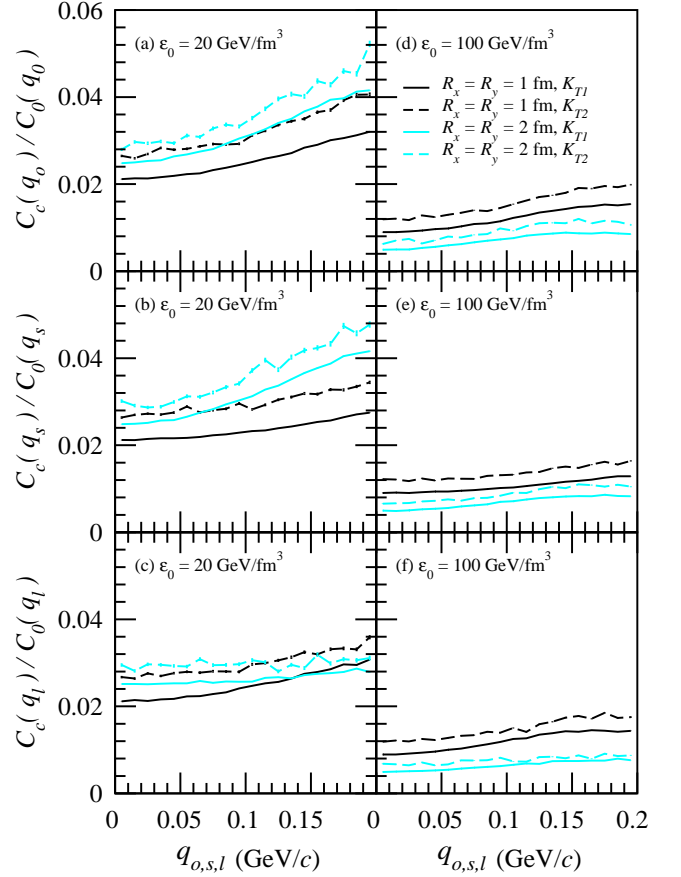


FIG. 3: The ratio of  $C_c$  to  $C_0$  for out (top panel), side (middle panel) and long direction (bottom panel). The results for the marks of  $K_{T1}$  and  $K_{T2}$  are calculated in the momentum regions  $0.2 \text{ GeV}/c \leq K_T \leq 0.4 \text{ GeV}/c$  and  $0.4 \text{ GeV}/c \leq K_T \leq 0.6 \text{ GeV}/c$ . Solid lines depict the results for  $K_{T1}$ , and the dashed lines depict the results for  $K_{T2}$ .

In Fig. 3, we show the ratio of  $C_c$  to  $C_0$  for out (top panel), side (middle panel) and long direction (bottom panel). Where the  $C_c$  is the corrected part of the correlation function. The results for the marks of  $K_{T1}$  and  $K_{T2}$  are calculated in the momentum regions  $0.2 \text{ GeV}/c \leq K_T \leq 0.4 \text{ GeV}/c$  and  $0.4 \text{ GeV}/c \leq K_T \leq 0.6 \text{ GeV}/c$ . Solid lines depict the results for  $K_{T1}$ , and the dashed lines depict the results for  $K_{T2}$ . Here, the ratio can quantitatively represent the volume effect on the correlation function. The Fig. 2 and Fig. 3 present the following four phenomena:

**I.** The correlation functions are more suppressed by the volume effect for  $\epsilon_0 = 20 \text{ GeV}/\text{fm}^3$  than for  $\epsilon_0 = 100 \text{ GeV}/\text{fm}^3$ .

**II.** For  $\epsilon_0 = 20 \text{ GeV}/\text{fm}^3$ , the correlation functions are more suppressed for  $R_x = R_y = 2 \text{ fm}$  than  $R_x = R_y = 1 \text{ fm}$  (see Fig. 2 (a)-(c)).

**III.** For  $\epsilon_0 = 100 \text{ GeV}/\text{fm}^3$ , the correlation functions are more suppressed for  $R_x = R_y = 1 \text{ fm}$  than  $R_x = R_y = 2 \text{ fm}$ .

2 fm (see Fig. 2 (d)-(f)).

**IV.** For a fixed initial condition, the volume effect on the correlation function for high momentum is greater than for lower momentum.

With the Bjorken boost-invariant hypothesis [18], the pion emission time and the longitudinal coordinate were expressed as

$$t = \tau \cosh \eta_s, \quad (12)$$

$$z = \tau \sinh \eta_s, \quad (13)$$

for a fixed spatial rapidity  $\eta_s$ , the pion emission time  $t$  and the longitudinal coordinate are proportional to the emission time in the  $z = 0$  plane. And the width of the time  $t$  and the longitudinal coordinate increase with the increasing spatial rapidity  $\eta_s$  for a fixed distribution of the  $\tau$ .

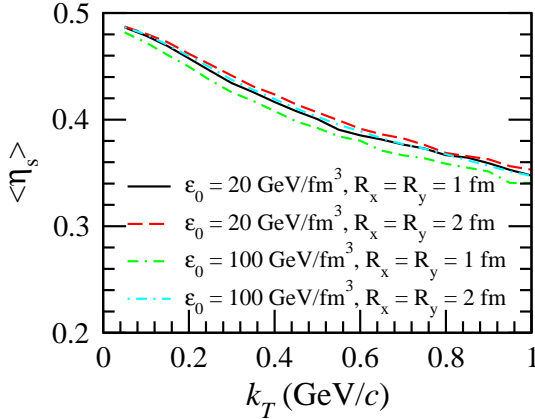


FIG. 4: The average emission spatial rapidity of the pion for different transverse momenta.

In Fig. 4, we show the average emission spatial rapidity of the pion for different transverse momenta. For a fixed transverse momentum, the average emission spatial rapidity of the pion varies little under different initial conditions. Thus, the main factor for phenomenon **I.** is that the width of the space-time distributions of the pion source in the  $z = 0$  plane for  $\epsilon_0 = 20 \text{ GeV/fm}^3$  are narrower than for  $\epsilon_0 = 100 \text{ GeV/fm}^3$  (see table I). For  $\epsilon_0 = 20 \text{ GeV/fm}^3$ , the transverse spatial width parameter,  $\sigma_r$ , of the pion source for  $R_x = R_y = 1 \text{ fm}$  is a little smaller than for  $R_x = R_y = 2 \text{ fm}$ . However, the temporal width parameter,  $\sigma_\tau$ , of the pion source for  $R_x = R_y = 1 \text{ fm}$  is much greater than for  $R_x = R_y = 2 \text{ fm}$ . Thus, the width of the time and the longitudinal space for  $R_x = R_y = 2 \text{ fm}$  are much narrower than for  $R_x = R_y = 1 \text{ fm}$ . And it is the main factor for phenomenon **II.** For  $\epsilon_0 = 100 \text{ GeV/fm}^3$ , the width of the space-time distributions of the pion source in the  $z = 0$  plane for  $R_x = R_y = 1 \text{ fm}$  are narrower than  $R_x = R_y = 2 \text{ fm}$  (see table I). And it is the main factor for phenomenon **III.**

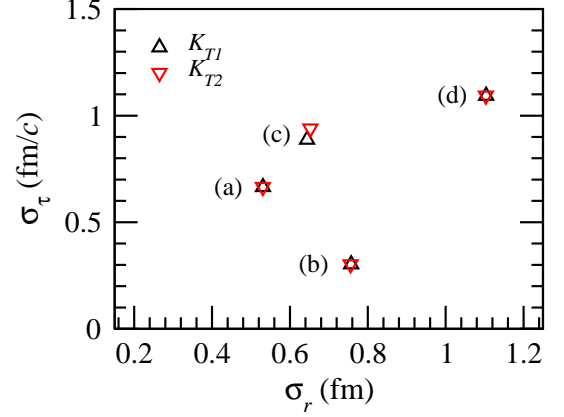


FIG. 5: The width parameters of time and space of the pion source in the  $z = 0$  plane for various initial conditions. The marks (a) - (d) represent the initial conditions are as the same as in Fig. 2.

In Fig. 5, we show the width parameters of time and space of the pion source in the  $z = 0$  plane for various initial conditions. The marks (a) - (d) represent the initial conditions are as the same as in Fig. 2. For a fixed initial condition, the width parameters of time and space of the pion source in the  $z = 0$  plane for different momenta are almost the same. The average emission spatial rapidity of the pion decreases with the increasing transverse momentum (see Fig. 4). Thus, the width of the time and the longitudinal space are narrower for large transverse momentum, and it leads to a greater volume effect on correlation function of the large transverse momentum (phenomenon **IV.**).

For a fixed initial condition, the correlation functions for high transverse momenta are more suppressed by the volume effect. Hence the incoherence parameter  $\lambda$  [1–4] may be more suppressed by the volume effect for high transverse momenta. Theoretically the incoherence parameter  $\lambda$  can be less than unity due to partial coherence of strong interaction, long-lived resonance decays and the non-Gaussian form of the correlation function [2, 4, 29–31]. Since for increasing transverse momenta the resonance contributions decrease, the  $\lambda$ -parameter increases with transverse momenta [30, 32–34]. For small collision systems, the volume effect is obvious, and it may lead to a small slope of the  $\lambda$ -parameter with respect to the transverse momentum.

#### IV. SUMMARY

Hadrons formed in heavy-ion collisions are not point-like objects, they cannot occupy too close space-time points. When the two bosons are too close to each other, their constituents start to mix and they cannot be considered as bosons subjected to Bose-Einstein statistics, this effect is called excluded volume effect [9–11].

In this paper, we study the volume effect on HBT for the sources with various sizes. The effect on HBT was shown in out, side and long directions, and it is more obvious for the source with a narrow space-time distribution. For a fixed initial condition, the correlation functions for high transverse momenta are more suppressed by the volume effect. And the incoherence parameter may be more suppressed by the volume effect for high transverse momenta. Hence it may lead to a small slope of the  $\lambda$ -parameter with respect to the transverse momentum for small collision systems.

## Acknowledgments

This research was supported by the National Natural Science Foundation of China under Grant No. 11647166, the Natural Science Foundation of Inner Mongolia under Grant No. 2017BS0104, Changzhou Science and Technology Bureau CJ20180054, and the Foundation of Jiangsu University of Technology under Grant No. KYY17028, KYY18048.

- 
- [1] C. Y. Wong, *Introduction to High-Energy Heavy-Ion Collisions* (World Scientific, Singapore, 1994), Chap. 17.
  - [2] U. Wiedemann, U. Heinz, Phys. Rept. **319**, 145 (1999).
  - [3] R. M. Weiner, Phys. Rept. **327**, 249 (2000).
  - [4] M. A. Lisa, S. Pratt, R. Soltz, and U. Wiedemann, Ann. Rev. Nucl. Part. Sci. **55**, 357 (2005).
  - [5] M. Acchiari et al. [L3 coll.] Phys. Lett. B **458**, 517 (1999); P. Achard et al. [L3 coll.], Eur. Phys. J. C **71**, 1648 (2011).
  - [6] G. Abbiendi et al. [OPAL coll.], Eur. Phys. J. C **16**, 423 (2000); P. Abreu et al. [DELPHI coll.] Phys. Lett. B **471**, 460 (2000); A. Heister et al. [ALEPH coll.] Eur. Phys. J. C **36**, 460 (2004).
  - [7] M. M. Aggarwal et al. (STAR Collaboration), Phys. Rev. C **83**, 064905 (2011).
  - [8] V. Khachatryan et al. [CMS coll.], JHEP **1105**, 029 (2011); L. Perroni, PoS (WPCF2011) 015.
  - [9] R. Hagedorn, J. Rafelski, Phys. Lett. B **97**, 136 (1980).
  - [10] G. D. Yen, M. I. Gorenstein, W. Greiner, S. N. Yang, Phys. Rev. C **56**, 2210 (1997).
  - [11] D. H. Rischke, M. I. Gorenstein, H. Stoecker, W. Greiner, Z. Phys. C **51**, 485 (1991).
  - [12] A. Bialas, K. Zalewski, Phys. Lett. B **727**, 182 (2013).
  - [13] A. Bialas, W. Florkowski, K. Zalewski, Phys. Lett. B **748**, 9 (2015).
  - [14] A. Bialas, EPJ Web of Conferences **120**, 01004 (2016).
  - [15] P. J. Siemens and J. O. Rasmussen, Phys. Rev. Lett. **42**, 880 (1979).
  - [16] E. Schnedermann, J. Sollfrank and U. Heinz, Phys. Rev. C **48**, 2462 (1993).
  - [17] W. Florkowski and W. Broniowski, Acta Phys. Polon. B **35**, 2895 (2004).
  - [18] J. D. Bjorken, Phys. Rev. D **27**, 140 (1983).
  - [19] C. Shen, U. Heinz, P. Huovinen, H. C. Song, Phys. Rev. C **82**, 054904 (2010).
  - [20] Q. H. Zhang, U. Wiedemann, C. Slotta, U. Heinz, Phys. Lett. B **407**, 33 (1997).
  - [21] S. Pratt, Phys. Rev. C **56**, 1095 (1997).
  - [22] D. Anchishkin, U. Heinz, P. Renk, Phys. Rev. C **57**, 1428 (1998).
  - [23] M. I. Gorenstein, V. K. Petrov and G. M. Zinovev, Phys. Lett. B **106**, 327 (1981).
  - [24] F. Cooper and G. Frye, Phys. Rev. D **10**, 186 (1974).
  - [25] B. R. Schlei, U. Ornik, M. Plumer, and R. M. Weiner, Phys. Lett. B **293**, 275 (1992).
  - [26] S. Chapman and U. Heinz Phys. Lett. B **340**, 250 (1994).
  - [27] C. Plumberg, U. Heinz Phys. Rev. C **91**, 054905 (2015).
  - [28] Y. Hu, W. N. Zhang, Y. Y. Ren, J. Phys. G: Nucl. Part. Phys. **42**, 045105 (2015).
  - [29] J. Adams et al. (STAR Collaboration), Phys. Rev. Lett. **93**, 012301 (2004).
  - [30] J. Adams et al. (STAR Collaboration), Phys. Rev. C **71**, 044906 (2005).
  - [31] Z. Q. Zhang, S. Zhang, and Y. G. Ma, Chin. Phys. C **38**, 014102 (2014).
  - [32] B. R. Schlei et al., Phys. Lett. B **293**, 275 (1992).
  - [33] J. Bolz et al., Phys. Lett. B **300**, 404 (1993).
  - [34] T. Csörgő, B. Lörstad, and J. Zimányi, Z. Phys. C **71**, 491 (1996).